

# BEAM-BEAM SIMULATIONS WITH THE GAUSSIAN CODE TRS

Miguel A. Furman<sup>\*†</sup>

Lawrence Berkeley National Laboratory, MS 71-259  
Berkeley, CA 94720, USA

Abstract

We describe features of the soft-gaussian beam-beam simulation code “TRS” and present sample results for the PEP-II  $e^+e^-$  collider.

## 1 DESCRIPTION OF THE CODE

A basic experimental observation in  $e^+e^-$  colliders in stable operation is that the particle distribution density at the beam core is approximately gaussian, while the density at large amplitudes (a few  $\sigma$ 's away from the center) is not gaussian and is much larger than the extrapolation from a gaussian fit to the core [1, 2].

The code TRS (Two-Ring Simulation) [3] is geared to study the beam core of colliding  $e^+e^-$  beams. Although it can be used to study large-amplitude tail distributions, it is very inefficient at doing so, since the vast majority of the CPU time is spent simulating the gaussian core. The “engine” of this code is similar to that in other codes [4, 5, 6, 7]. The code is written in FORTRAN 77, and is yet to be documented in detail.

### 1.1 Simulation technique

In the simplest case each beam is represented by a single bunch traveling in a separate, distinct ring and collisions occur at only one interaction point (IP). The basic simulation technique consists in tracking a given number (typically 1000–50000) of macroparticles per bunch and computing, at every turn just before the collision, the centroids  $\langle x \rangle_{\pm}$ ,  $\langle y \rangle_{\pm}$  and rms widths  $\sigma_{x\pm}$ ,  $\sigma_{y\pm}$  of the distributions, where the subscript  $+$ ( $-$ ) refers to the  $e^+$ ( $e^-$ ) beam. For the purposes of computing the beam-beam interaction, the code assumes that the transverse distribution of the kicking bunch is gaussian, using the just-computed values of  $\langle x \rangle$ ,  $\langle y \rangle$ ,  $\sigma_x$  and  $\sigma_y$  in the Bassetti-Erskine formula [8] for the electromagnetic field of a gaussian distribution. This formula is then used to compute the kick on every macroparticle of the opposing bunch. The role of the two colliding bunches is then reversed, completing the computation of the beam-beam interaction.

Each macroparticle is then tracked through its corresponding ring lattice, and the process is iterated for many turns, typically corresponding to 3–5 damping times. An aperture “lattice element” intercepts par-

ticles at large amplitude, and these are removed from the simulation.

The main output of the program is a file the with turn-by-turn values of  $\langle x \rangle_{\pm}$ ,  $\langle y \rangle_{\pm}$ ,  $\sigma_{x\pm}$ ,  $\sigma_{y\pm}$  and the remaining number of macroparticles. Simple post-processors can then compute the luminosity and the frequency spectra of  $\langle x \rangle_{\pm}$ ,  $\langle y \rangle_{\pm}$ ,  $\sigma_{x\pm}$  and  $\sigma_{y\pm}$ . The program can also output the  $x$  and  $y$  projections of the time-averaged macroparticle distributions in binned form.

### 1.2 Other features

Nonzero bunch-length effects are taken into account by slicing the bunch longitudinally, so that the beam-beam interaction is represented by several kicks [9] with prescribed locations and weights. In the simplest case (thin-lens approximation) there is a single kick at the center of the bunch. Typically, however, one uses a thick-lens approximation with 5 or more kicks. In between two consecutive kicks, the macroparticles undergo simple drifts as they pass through the opposing bunch. The program only allows for head-on collisions (zero crossing angle), although the centers of the beams are allowed to be offset.

The particle kinematics is fully 6-dimensional; however, the longitudinal component of the beam-beam kick is wholly ignored, which is typically a good approximation. The synchrotron motion of the particles can be chosen to be parametric, i.e. an exact harmonic rotation with a specified synchrotron tune, or can be implemented with an RF cavity kick plus a time-of-flight “lattice element” which is a function of the (specified) momentum compaction factor.

The parameters of the two beams and the two rings are fully independent of each other. The ring lattices can contain arbitrary nonlinear thin elements, apertures, or linear phase-advance maps. In typical applications, however, the entire ring is represented by a simple linear map with specified tunes plus a rectangular aperture.

Radiation damping and quantum excitation are also represented by simple kick elements that typically act once per turn. These elements are constructed so that, in the absence of the beam-beam interaction, the rms beam sizes  $\sigma_{x\pm}$  and  $\sigma_{y\pm}$  would reach specified values  $\sigma_{0x\pm}$  and  $\sigma_{0y\pm}$  after many damping times, regardless of the initial conditions.

Parasitic collisions can be included by an appropriate lattice element whose strength depends on the pa-

---

<sup>\*</sup> Work supported by the US Department of Energy under contract No. DE-AC03-76SF00098.

<sup>†</sup> mafurman@lbl.gov

rameters of the opposing bunch.

The code can run in “weak-strong” mode, “strong-strong” mode, or single-particle tracking mode. In the weak-strong mode, one beam (the strong beam) is represented by a static gaussian lens (thin or thick) with specified, unchanging,  $\sigma$ 's, and the other beam (the dynamical, or weak, beam) by a collection of dynamical macroparticles. In strong-strong mode both beams are represented by macroparticles whose distributions vary dynamically under their mutual beam-beam interaction. Single-particle tracking mode is the same as weak-strong mode in which the weak beam consists of a single particle. In this case the output from the program is the turn-by-turn phase space of this particle. This mode is used to study single-particle resonance effects and to produce beam-beam footprints; it has also proven valuable in debugging the code and in allowing for basic comparisons with other codes and with analytic results.

The code also offers choices of algorithms for the computation of the complex error function, which enters the Bassetti-Erskine formula. Typically we use a 3rd-order table interpolation [10], but one can also use a 4th-order interpolation, a Padé approximant [11], or the IMSL<sup>®</sup> function CERFE [12]. Similarly, the program offers the choice of several slicing algorithms to assign the locations and weights of the kicks representing the long-bunch effects, and also two algorithms for the computation of radiation damping and quantum excitation effects.

### 1.3 Tests

The program has been systematically tested against analytic results in single-particle mode, and against other similar simulation codes in their common region of applicability [13, 14]. In single-particle mode, the excellent agreement with analytic results of the amplitude-dependent tune shift validates the basic beam-beam force computation. In weak-strong mode, minor disagreements with other codes can be attributed to differences in details of the codes other than the beam-beam computation.

### 1.4 Speed

In the typical case when the lattice is represented by a linear map, the CPU time used by the program is dominated by the beam-beam computation. For a given run, the CPU time scales according to

$$\text{CPU time} \propto (\text{no. of macroparticles/bunch}) \times (\text{no. of slices}) \times (\text{no. of turns}) \quad (1)$$

A rough idea of the program speed is obtained from informal benchmarks on three computers: in units of CPU-sec/(macroparticle $\times$ slice $\times$ turn), the speed (or, rather, the inverse speed) is  $2.1 \times 10^{-5}$ ,  $1.3 \times 10^{-5}$  and  $8.7 \times 10^{-5}$  on NERSC's C90 Cray computer, on

NERSC's T3E computer “mcurie” in single-processor mode, and on a Sun SPARCstation 20, respectively. These numbers assume that the beams collide once per turn, that both are represented by the same number of macroparticles, and that the complex error function is computed via a 3rd-order table interpolation algorithm.

The above speeds are for strong-strong mode; in weak-strong mode, the program runs roughly twice as fast, as it should be expected.

### 1.5 Drawbacks

Although the gaussian approximation has the advantage of simplicity, its accuracy relies on the assumption that the core of the distribution is gaussian. However, it should be kept in mind that, in certain cases, depending on the values of the tunes and the beam-beam parameters, coherent single-bunch resonances can appear that distort the core distribution significantly away from the gaussian shape. In this case, obviously, the Bassetti-Erskine formula is not expected to be reliable. A more adequate solution is provided by a PIC code in which the electromagnetic kick is computed from the actual macroparticle distribution [15, 16].

Nevertheless, the gaussian approximation is reliable in many cases of practical interest. And, as shown in the examples below for PEP-II, even if the conditions are such that a coherent resonance appears, the gaussian approximation behaves qualitatively differently from the “normal” case, providing a signal that the gaussian approximation should be suspect.

## 2 APPLICATION TO PEP-II

The code TRS has been applied to the PEP-II collider to obtain tune scans whose primary goal is to establish areas in the tune plane with acceptable luminosity performance [17]. For the purposes of this article we use a model of the machine in which the rings are represented by linear arcs of specified tunes, and parasitic collisions are ignored. Table 1 provides a basic parameter list used in the simulations.  $E$  is the nominal beam energy,  $N$  is the number of particles per bunch, the  $\xi_0$ 's are the nominal beam-beam parameters, the  $\beta^*$ 's and  $\sigma_0^*$ 's are the optics functions and nominal beam sizes at the interaction point (IP), respectively, the  $\tau$ 's are the damping times, and the  $\nu_s$ 's are the synchrotron tunes.

Fig. 1 shows the time evolution of the normalized rms beam sizes for the tune values shown. The simulation was run for 25000 turns, i.e.,  $\sim 3 e^+$  damping times, with 50000 macroparticles per bunch using 5 kicks for the bunch length effects. The beam sizes start out being smaller than the nominal sizes owing to the dynamical  $\beta$  effect [18], and the beam blowup behavior is typical of incoherent resonance effects.

Table 1: Basic PEP-II parameters.

	$e^+$	$e^-$
$E$ [GeV]	3.1	9.0
$N$ [ $10^{10}$ ]	5.685	1.958
$\xi_{0x}$	0.03	0.03
$\xi_{0y}$	0.03	0.03
$\beta_x^*$ [cm]	50	50
$\beta_y^*$ [cm]	1.5	1.5
$\sigma_{0x}^*$ [ $\mu\text{m}$ ]	153.0	153.0
$\sigma_{0y}^*$ [ $\mu\text{m}$ ]	4.591	4.591
$\sigma_z$ [cm]	1.0	1.0
$\nu_s$	0.0334	0.0521
$\tau_x = \tau_y$ [turns]	8366	5014

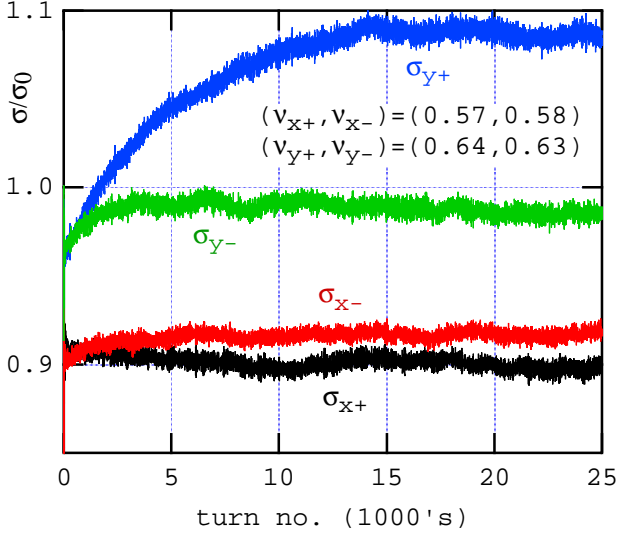


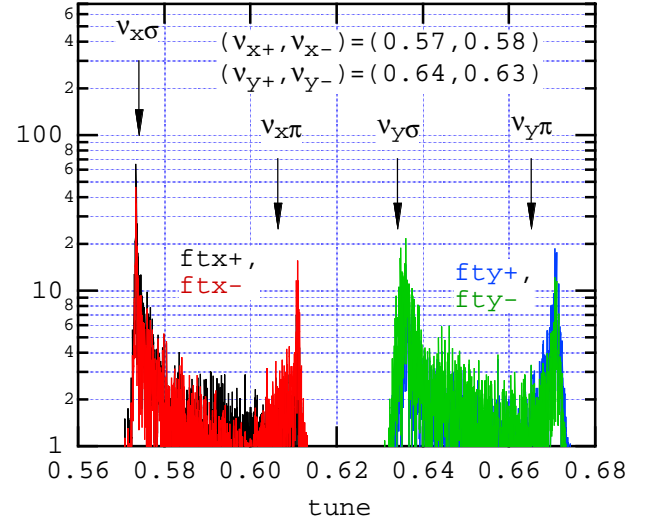
Figure 1: Time evolution of the normalized rms beam sizes for split tunes.

Fig. 2 shows the spectra, in absolute value, of the horizontal and vertical oscillations of the beam centroid for both beams. The arrows indicate the tunes of the  $\sigma$  and  $\pi$  modes computed in the rigid-gaussian small-amplitude approximation, given by [19]

$$\cos \left\{ \frac{2\pi\nu_\pi}{2\pi\nu_\sigma} \right\} = \frac{1}{2}(C_+ + C_-) - \pi(S_+\Xi_+ + S_-\Xi_-) \pm \sqrt{R}, \quad (2)$$

$$R \equiv \frac{1}{4}(C_+ - C_-)^2 + \pi^2(S_+\Xi_+ + S_-\Xi_-)^2 - \pi(C_+ - C_-)(S_+\Xi_+ - S_-\Xi_-) \quad (3)$$

Here the subscript  $+$ ( $-$ ) refers to the  $e^+$ ( $e^-$ ) beam,  $C_\pm \equiv \cos 2\pi\nu_\pm$ ,  $S_\pm \equiv \sin 2\pi\nu_\pm$ , the  $\nu$ 's are the tunes and the  $\Xi$ 's are the coherent beam-beam parameters [20]. For example, the horizontal coherent beam-beam


 Figure 2: Absolute value of the tune spectra, in arbitrary units, of the centroid motions of the two beams for split tunes. The spectra of the two beams almost exactly overlap. The arrows indicate the  $\sigma$  and  $\pi$  tunes computed from Eqs. (2-4).

parameter of the positron beam is

$$\Xi_{x+} = \frac{r_e N_- \beta_{x+}^*}{2\pi\gamma_+ \Sigma_x (\Sigma_x + \Sigma_y)} \quad (4)$$

with corresponding expressions for  $\Xi_{x-}$  and  $\Xi_{y\pm}$ . Here  $r_e$  is the classical electron radius,  $\gamma$  is the usual relativistic factor and  $\Sigma_x = (\sigma_{x+}^{*2} + \sigma_{x-}^{*2})^{1/2}$  with a similar expression for  $\Sigma_y$ .

The  $\sigma$  and  $\pi$  tunes shown by the arrows in Fig. 2 take into account the equilibrium beam sizes in Eq. (4), obtained from Fig. 1. The disagreement of  $\nu_\pi$  with the second peak of the simulated spectra can be explained by the fact that the bunches are not rigid but rather vary dynamically in shape and size [21, 22].

Fig. 3 shows the spectra of the rms beam sizes. The signals of the synchrotron tunes, labeled  $\nu_{s\pm}$ , are clearly seen. Simulations not shown here indicate that, when the tunes are slightly changed, the main peaks move at twice the rate of change of the tunes [23].

If the tunes are chosen pairwise equal, a qualitatively different result obtains. Fig. 4 shows the time evolution of the rms beam sizes for  $\nu_{x+} = \nu_{x-} = 0.57$  and  $\nu_{y+} = \nu_{y-} = 0.64$ . After a transition at  $\sim 5000$  turns, corresponding to the damping time of the  $e^-$  beam, the vertical beam sizes of the two beams are locked together and blow up to a larger value than in the split-tune case. Another feature of the dynamics is shown in Fig. 5, in which the normalized vertical beam sizes are plotted for only 20 consecutive turns. When the starting turn is 2000, the beam sizes are uncorrelated, while if the starting turn is 20000, the sizes are correlated and oscillate in phase with period 3. These behaviors are typical of coherent beam-beam resonances which

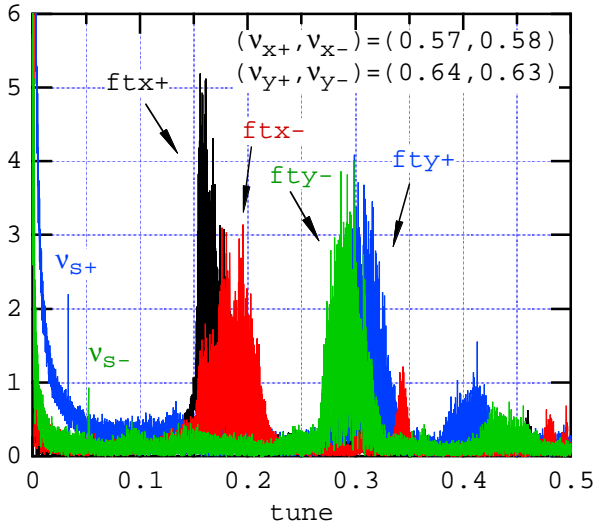


Figure 3: Absolute value of the rms beam size spectra in arbitrary units for split tunes.

can be studied in more quantitative detail by other means, as discussed in Sec. 1.5. In practice, a more realistic simulation of PEP-II requires the inclusion of the parasitic collisions near the IP [17]. These collisions, although relatively weak, are sufficiently strong to destroy the coherent resonance condition, and the actual behavior observed in the simulation is of the “normal” kind, i.e., dominated by incoherent effects, as in the split-tunes example discussed earlier.

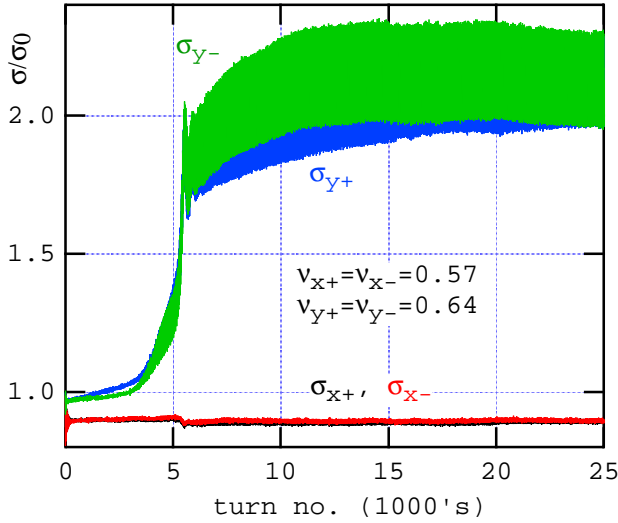


Figure 4: Time evolution of the normalized rms beam sizes for pairwise-equal tunes.

### 3 SUMMARY

We have summarized the main features of the beam-beam simulation code TRS and presented two sample applications to the PEP-II collider. The code has been

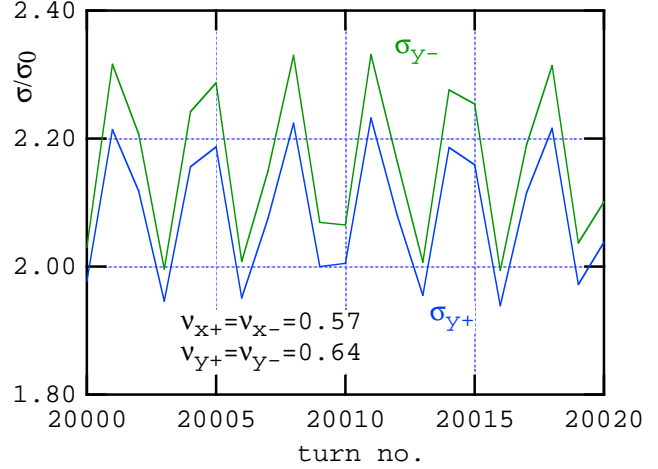
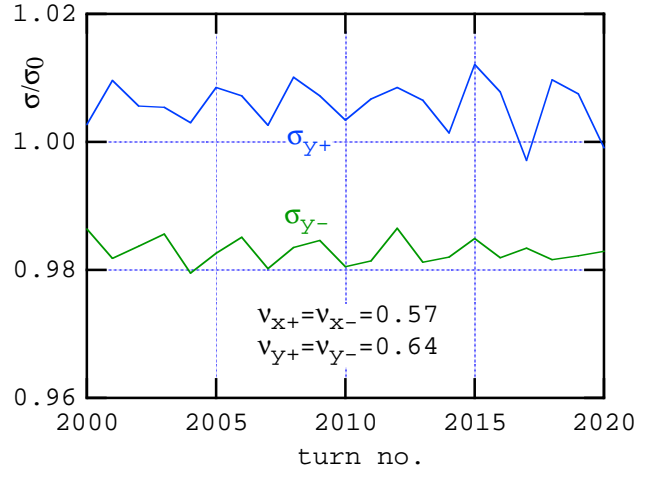


Figure 5: Detail from Fig. 4: time evolution for 20 consecutive turns of the normalized vertical rms beam sizes. Top: starting at turn 2000; bottom: starting at turn 20000.

successfully tested against analytic results and against other simulation codes whenever such comparisons are meaningful.

The soft-gaussian approximation is believed to represent reliably incoherent beam-beam effects. The code has been used to perform studies for the PEP-II collider. For example, simulated tune scans reveal undesirable operating points due to beam blowup from synchrotron sidebands. The dynamical beta effect, clearly seen in these simulations, also influences the choice of a working point. The code has been used to establish the adequate beam separation at the parasitic collision points [24], and has been applied to the proposed muon collider [25], including the effects from the instability of the muon.

In some cases the code clearly reveals coherent behavior; however, the soft-gaussian approximation is quantitatively unreliable in such cases, and other methods are called for.

Present improvement plans include allowing for non-

linear maps to better represent the machine lattice, and for collisions at a crossing angle.

#### 4 ACKNOWLEDGMENTS

I am grateful for many discussions and/or collaboration over time with E. Anderson, A. Chao, T. Chen, Y. H. Chin, J. Eden, E. Forest, W. Herr, K. Hirata, J. Irwin, S. Krishnagopal, E. Keil, R. Li, K. Y. Ng, D. Shatilov, R. Siemann, J. Tennyson, K. Yokoya and A. Zholents.

#### 5 REFERENCES

- [1] J. T. Seeman, "Observations of the Beam-Beam Interaction," Proc. Nonlinear Dynamics Aspects of Particle Accelerators, Sardinia, January 31–February 5, 1985, Springer Verlag Lecture Notes in Physics 247, p. 121.
- [2] D. Rice, "Observations of the Beam-Beam Effect in PEP, SPEAR and CESR," Proc. Third Advanced ICFA Beam Dynamics Workshop (Beam-Beam Effects in Circular Colliders), I. Koop and G. Tumaikin, eds., Novosibirsk, May 29–June 3, 1989, p. 17.
- [3] J. L. Tennyson, undocumented code "TRS," 1989.
- [4] S. Myers, "Review of Beam-Beam Simulations," Proc. Nonlinear Dynamics Aspects of Particle Accelerators, Sardinia, January 31–February 5, 1985, Springer Verlag Lecture Notes in Physics 247, p. 176.
- [5] K. Yokoya and Y. H. Chin, undocumented code.
- [6] K. Hirata, "Analysis of Beam-Beam Interactions with a Large Crossing Angle," Phys. Rev. Lett. 74, 2228 (1995).
- [7] E. B. Anderson and J. T. Rogers, "ODYSSEUS: A Dynamic Strong-Strong Beam-Beam Simulation," CBN 97-33, November 9, 1997, and these proceedings.
- [8] M. Bassetti and G. A. Erskine, "Closed Expression for the Electric Field of a Two-Dimensional Gaussian Charge," CERN-ISR-TH/80-06.
- [9] S. Krishnagopal and R. Siemann, "Bunch-Length Effects in the Beam-Beam Interaction," Phys. Rev. D41, p. 2312 (1990).
- [10] Handbook of Mathematical Functions, M. Abramowitz and I. A. Stegun, Eds., Dover Publications Inc., 9th printing, 1970.
- [11] Y. Okamoto and R. Talman, "Rational Approximation of the Complex Error Function and the Electric Field of a Two-Dimensional Charge Distribution," CBN 80-13, Sept. 1980.
- [12] IMSL Math/Library<sup>®</sup> Reference Manual, v. 10.0.
- [13] M. A. Furman, A. Zholents, T. Chen and D. Shatilov, "Comparisons of Beam-Beam Code Simulations", CBP Tech Note-59/PEP-II AP Note 95.04, July 13, 1995.
- [14] M. A. Furman, A. Zholents, T. Chen and D. Shatilov, "Comparisons of Beam-Beam Simulations," Proc. Seventh Advanced ICFA Workshop on Beam Dynamics, JINR, Dubna, Russia, 18-20 May 1995, (P. Beloshitsky and E. Perelstein, eds.), p. 123.
- [15] S. Krishnagopal and R. Siemann, "Coherent Beam-Beam Interaction in Electron-Positron Colliders," Phys. Rev. Lett. 67, pp. 2461–2464 (1991).
- [16] S. Krishnagopal, "Luminosity-Limiting Coherent Phenomena in Electron-Positron Colliders," Phys. Rev. Lett. 76, pp. 235–238 (1996).
- [17] "PEP-II: An Asymmetric B Factory - Conceptual Design Report," June 1993, LBL-PUB-5379/SLAC-418/CALT-68-1869/UCRL-ID-114055/ UC-IIRPA-93-01.
- [18] M. A. Furman, "Beam-Beam Tune Shift and Dynamical Beta Function in PEP-II," Proc. European Particle Accelerator Conference, London, England, June 27–July 1, 1994, p. 1145.
- [19] K. Hirata and E. Keil, "Coherent Beam-Beam Interaction Limit in Asymmetric Ring Colliders," Phys. Lett. B232, 413 (1990).
- [20] K. Hirata, "Coherent Betatron Oscillation Modes Due to the Beam-Beam Interaction," NIM A269, 7 (1988).
- [21] R. E. Meller and R. H. Siemann, "Coherent Normal Modes of Colliding Beams," IEEE Trans. Nucl. Sci. NS-28 No. 3, 2431 (1981).
- [22] K. Yokoya, Y. Funakoshi, E. Kikutani, H. Koiso and J. Urakawa, "Tune Shift of Coherent Beam-Beam Oscillations," KEK Preprint 89-14; K. Yokoya and H. Koiso, Part. Accel. 27, pp. 181–186 (1990).
- [23] I am indebted to E. Keil for discussions and for unpublished results on this point.
- [24] M. A. Furman, "Parasitic Collisions in PEP-II," Proc. Seventh Advanced ICFA Workshop on Beam Dynamics, JINR, Dubna, Russia, 18-20 May, 1995 (P. Beloshitsky and E. Perelstein, eds.), p. 36.
- [25] M. A. Furman, "The Classical Beam-Beam Interaction for the Muon Collider: A First Look," LBL-38563/BF-19/CBP Note-169, April 25, 1996, Proc. 1996 Snowmass Workshop "New Directions for High-Energy Physics."